SPECTROSCOPIC STUDY OF BARIUM STARS

Ashok. D, Monish. R, Munagala Reddy Charan Reddy
Research Internship fellow,
Indian Institute of Astrophysics, Bengaluru.
Department of Aerospace Engineering,
Alliance University,
Bengaluru, Karnataka, INDIA.

Abstract: **We present the abundance results from the high-resolution spectral analysis of fifteen barium stars. The spectral resolution is R ~ 86000 with a wave length coverage of 3900 – 9000 °A. Stellar atmospheric parameters the effective temperature, surface gravity, metallic ties are determined from the local thermodynamic equilibrium analys is using model atmospheres. The effective temperature of the programme stars ranges from 3535 – 7656 K. The surface gravity covers a range from 1.17 – 4.07 cgs and metallicity ranges from -1.41 to - 0.13.We have also obtained temperature from photometric calculations and log g from parallax method. These values are found to match closely with the spectroscopic values within errors. The elemental abundances are determined from the spectrum synthesis calculation of clean and unblended lines due to neutral and ionized elements using iSpec. The abundances of elements such as O, Na, Mg, Ca, Sc, Ti, Mn, Ni, Cu, Zn, Sr, Y, Zr, Ba, La, Ce, Nd, Pr, Sm and Eu are determined. The star HD 22589 shows enhancement in Ba with [Ba/Fe] > 1.33. HD 40430 is found to be Ba normal with [Ba/Fe]0.10.The mass and the age of the programme stars are also determined from their locations in the H-R diagram. The estimated mass of the programmestars ranges from 1.20-4.50M⊙ and age from 0.53to3.36Gyr.**

I. INTRODUCTION

Barium stars are chemically peculiar stars that show enhancement of neutron-capture elements. Barium stars are population I objects with spectral class F and K and were first identified by Bidel man and Keenan (1951). The spectra of the Bastarss how strong lines of Ba II at 4554°Aand SrII at 4077 A. Bastars are mostly found in the disc of our galaxy and found to exhibit radial velocity variations (Mc Clureetal., 1980; McClure1983, 1984) through long-term radial velocity monitoring programs of Bastars.

The widely accepted scenario to explain the observed enhancement of neutron-capture elements in barium stars is mass transfer from a binary companion. According to this scenario, the primary companion while at the Asymptotic Giant Branch (AGB) phase of evolution synthesized the heavy elements through slow neutron-capture process and the synthesized material were transferred to the secondary companion through some mass-transfer mechanisms such as the Roche-Lobe overflow or stellar wind. This leads to the observed enhancement of heavy elements in the secondary stars, i.e., the now observed Ba stars. The primary companion has further evolved from AGB phase of evolution to a now invisible white dwarf. The surface chemical composition studies of Ba stars can thus provide insight into the neutron-capture nucleosynthesis occurring in the AGB phase of evolution of low and intermediate mass stars. In this work, we have presented a detailed abundance analysis of fifteen Ba stars based on high-resolution spectroscopy. The report is organized as follows. In section 2, we have presented a brief summary of the previous works from literature on our programme stars. Section 3 presents the selection of objects, observation, and data reduction. Estimation of photometric temperature is presented in section 4. Details of the spectral analysis which includes the estimation of atmospheric parameters, mass and age of the stars are presented in section 5. Section 6 provides the details on the abundance analysis.Conclusions are drawn in section 7. The abundance pattern of elements and iron group follows the abundance pattern of the disk population and in particular the old-disk population.

II. PREVIOUS WORKS ON THE PROGRAM STARS: A SUMMARY

Some aspects of the programme stars under this study have been studied by different authors. In this section we briefly summarize their main results.

Jorissen et al (2019): These authors have conducted detailed study of the binary nature of Barium and related stars. 34 extrinsic S stars, 40 mild barium stars and 37 strong barium stars were photo metrically and spectroscopic ally monitored. They conclude in their work that Barium and S stars are red giants, and since these stars have overabundances in heavy elements they are

suspected to be in binary system. Their studies show that all their programme stars are confirmed binaries except HD 95345. In their study they have found out that the offset in the velocity between HERMES and Udry et al. (1999) for the star HD 18182 is to be 0.6 km/s with radial velocity varying from 24 – 25 km/s. Metallicity and radial velocity for the stars HD 40430, HD 53199, HD

98839, HD 183915, and HD 211954 were also reported. Other properties, such as period and the revised orbital elements, are reported for stars HD 18182, HD 119185, and HD 134698.

Allen Barbuy (2006): Detailed study of 26 barium stars are presented in this paper. The derived atmospheric parameters are in the range 4300 < T eff < 6500, -1.2 < [Fe/H] < 0.0 and 1.4 log g < 4.6. They have confirmed the existence of dwarf barium stars among their sample stars by deriving the luminosity classes and gravities of these stars. They have estimated a radial velocity 8.10 km/s for the star HD 87080. Estimates of T eff , micro turbulence, log g and metallicity for HD 22589, HD 76225, HD87080, HD 106191, HD 147609, and HD 150862, are presented in this paper. They have found excess of abundances for the elements Na, Al, Mg, Si and Ca relative to Fe in the range -0.2 to 0.2 dex. In this work they have obtained the barium abundance with respect to Fe is found to be enhanced with 0.8 [Ba/Fe] 1.80.

Pereira (2003) (2005): Based on the high-resolution optical spectra the abundance of HD 22589 along with two other barium dwarf stars are analysed in this work. Alternative synthetic spectra are shown to demonstrate the sensitivity of the line strength to the abundances. We could get good fits using the following method for the corresponding elements**.**

III. SOURCE OF SPECTRA ANALYSED IN THIS STUDY

High-resolution spectra for the objects under this study were acquired using the HERMES spectrograph (Raskin 2011) mounted on the 1.2m Mercator telescope at the Roque de los Muchachos Observatory, La Palma, Canary Islands. The spectra cover the wavelength range 3900- 9000 A at a resolution of R 86000. These objects were observed as part of a long-term monitoring of radial velocities to detect the binary nature and derive orbital parameters of specific families of stars. We have used co-added spectra, formed by co-adding various spectra from different nights, after correcting for the Doppler shifts to maximize signal-to-noise ratio (SNR). A Python- based pipeline was used to extract wavelength-calibrated, cosmic-ray cleaned spectrum. We have used some of these science ready spectra of the

respective objects for our de- tailed studies including abundance analysis.

The RV measurements and the derived orbital parameters for these objects can be found in Jorissen et al. (2019) and Escorza et al. 2019. The atmospheric parameters for these stars derived using the pipeline BACCHUS(Masseron 2016) in a semi-automated mode using interpolated MARCS model atmospheres (Gustafsson et al. 2008) and the 1D Local Thermo-dynamical Equilibrium (LTE) spectrum-synthesis code TURBOSPECTRUM (Al- varez et al. 1998, Plez et al. 2012) gave preliminary estimates of the parameters.
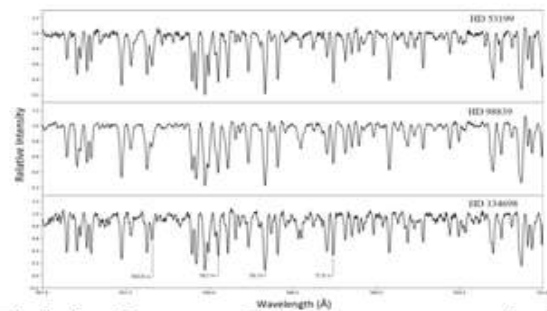

Fig 1. Sample spectra of a few programme stars in the wave-length region 5070 to 5100A.
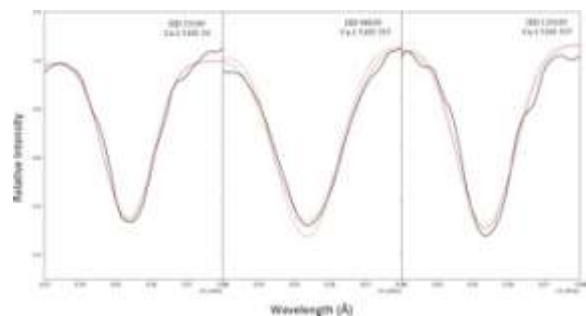
Fig 2. Spectral-synthesis fits of Cu I line at 5105.535 A is shown for three objects HD 53199, HD 98839 and HD 119185 in the plot. The dotted lines indicate the synthesized spectra and the solid lines indicate the observed line spectra. Two

IV. ESTIMATION OF PHOTOMETRIC TEMPERATURE

The bolometric luminosity of the star is given by L = 4R2T eff 4, where L is the luminosity, R is the radius of the star and T eff is the effective temperature of the star. The colour index of a star gives a measure of its temperature. The smaller the value of color index, the bluer (or hotter) the object is. To determine the color index of a star, the star must be observed through two different filters. The two filters generally used are U B and B V. These are ultraviolet (U), blue (B), and visible (V) filters, respectively. The value of U-B and

B-V gives the estimates of temperature of the star. These colour indices are dependent on the term called as interstellar extinction. Only the index called as true index is unaffected by the extinction, which is believed to be a hypothetical index. This extinction is nothing but the scattering of star's light through interstellar medium. The interstellar medium is filled with debris, gas, dust. These things very much fac- tor the scattering of a star's light. While the telescopes observe and analyses the star's data on the ground, the data are affected by the earth's atmosphere also. So, both the interstellar extinction and atmosphere of the earth effects the observed data.

The Photometric temperature of our programme stars are estimated using the calibration equations of Alonso et al. (1999, 2001) and following the detailed procedures as given in our earlier papers (Goswami et al. 2006, 2016). As our programme star sample consists of both main- sequence stars and giants, we have made use of the corresponding calibration equations separately for each group The temperature calibrations derived by Alonso et al. (1996), relate T eff with various optical and near-IR colours.

Alonso et al. estimate an external uncertainty in the temperature calculation using this method of 90 K. The Alonso calibrations of B-V, V-R, V-I, R-I and V-K require colours in the Johnson system, and the calibrations of the IR colours J-H, and J-K in the TCS system (the photometric system at the 1.54 m Carlos Sanchez telescope in Tenerife; Arribas Martinez-Roger 1987). To obtain the V-K colour in the Johnson system we first transformed the Ks 2MASS magnitude to the TCS system. Then, using eqs (6) and (7) of Alonso et al. (1994), K is transformed to the Johnson system from the TCS system. In order to transform the 2MASS colours J-H and J-KS onto the TCS system we first transformed the 2MASS colours to CIT colours (Cutri et al. 2003), and then from CIT to the TCS system (Alonso et al. 1994).

Estimation of the T eff from T eff - (J-H) and T eff - (V- K) relations also involves a metallicity ([Fe/H]) term. We have estimated the T eff of the stars at several metallicities. The estimated temperatures, along with the adopted metallicities, are listed in Table 1. The broadband B-V colour is often used for the determination of T eff , how- ever, the B-V colour of a star with strong molecular car- bon absorption features depends not only on T eff , but also on the metallicity of the star and on the strength of its molecular carbon absorption features, due to the effect of CH molecular absorption in the B band. For this reason, we have not used the empirical T eff scale for the B-Vcolour indices.

The temperatures listed in Table 1 span a wide range; while J-K, J-H, and V-K colours provide similar temperatures, the V-I colour predict higher temperatures. J, H, K magnitudes of the objects required for temperature estimates are taken from SIMBAD database which came from 2MASS (Cutri et al. 2003). We have used the estimated photometric temperatures as the initial guess for the estimation of spectroscopic temperature of the objects.

We have obtained the temperature estimates at three assumed metallicity values -0.05, -0.5, and -1.5. The J-K colour index does not depend on metallicity. For most of the stars HD 87080, HD 40430, HD 183915, HD 150862, HD 134698, HD 22589, HD 119185, HD 211594 the spectroscopic ally derived temperature estimates match with temperature estimates derived using (J-K)-T eff calibration within +/- 300 K, except for the star HD 95241. The rea- son for the star HD 95241 showing such a large difference (1820 K) is not understood clearly.

$$M_V = V - 5\log \frac{1}{distance} + 5$$

Where V is the color index of visual filter,

$$a = \frac{-9.930 * 0.01}{\log_{10}(T_{eff}) - 3.352}$$

$$x = \log_{10}(T_{eff}) - 3.52 \text{ The}$$

bolometric correction is calculated by,

$$BC = a + (2.887 * 0.01) + (3.375 * x) - (4.425 * x2) + (0.3505 * x * m)$$
$$- (5.558 * 0.01 * m) - (5.375 * 0.001 * m2)$$

Next, we must calculate the interstellar extension parameter

$$Av = Mv + BC - MB$$

The luminosity ratio is given by,

$$Log (L/L_\odot)$$

$$\frac{=4075 - MB}{2.5}$$

V.   SPECTRAL ANALYSIS

The analys is consists of the following steps:

5.1 LINEIDENTIFICATION

Lines due to neutral and ionized elements are identified by comparing the spectra with the spectrum of Arcturus using. We have used only clean and unblended lines for our analysis. The equivalent widths of these clean lines were measured. Many lines due to a same element were measured to get more accurate results. A master line list is prepared using the spectral information such as laboratory wavelength, excitation potential and log g values of the respective elements. The line information is taken from the Kurucz database of atomic line lists. (https://www.cfa.harvard.edu/amp/ampdata/ kurucz23/sekur.html).

5.2   Estimation of stellar mass surface gravity (LOGG)

We have estimated the mass of our programme stars from their position in the HR diagram,

log (L/L $\odot$) vs. spectroscopic T eff plots (Fig 3,4,5). Plot of luminosity versus temperature is called as Hertzsprung Russel diagram. We get trends of many stars which says about the evolutionary stage of the star. Most of the stars fall in a trend called as main sequence. The hotter a star is the more luminous it will be. So, understanding of the HR is essential to understand the properties of the star and its evolution. We know the mass to luminosity relation which says, L M 3.5 that means more luminous a star is, more massive it will be. In our galaxy, most of the stars are low mass objects. In the HR diagram the stars that lie in the upper left portion are higher mass, higher surface temperature, more luminous stars. The absolute visual magnitude of the star is calculated by,The mass of the star is an important predictor for many other characteristics, including how long it will live and the type of the star. The stars with higher masses will have shorter lifespan compared with the less massive stars. This is because the heavier stars consume its nuclear fuel faster than the lighter ones. The stars with high mass are much hotter than the stars with low masses. The required visual magnitudes V of the stars are taken from SIMBAD and the parallaxes are taken from Gaia (Gaia collaboration et al. 2016, 2018b, https://gea.esac.esa.int/archive/) whenever possible. The bolometric corrections are determined separately for main-sequence and subgiants/giants using the empirical calibrations of Alonso et al. (1999). Interstellar extinction (Av) for objects with Galactic latitude b < 50 degree are calculated based on formulae by Chen et al (1998). We

made use of Girardi et al. (2000) database (http://pleiadi.pd.astro.it/) of evolutionary tracks to estimate the mass of the stars. For near solar objects evolutionary tracks corresponding to Z = 0.019 are chosen. Surface gravity logg is calculated from the estimated mass using the relation

$$\log \frac{g}{g_\odot} = \log \frac{M}{M_\odot} + 4\log \frac{T_{eff}}{T_{eff\odot}} + 0.4(M_{bol} - M_{bol\odot})$$

The adopted values for the Sun are log g sun = 4.44, T eff sun = 5770K, and Mbol sun = 4.75 mag (Yang et al.2016). We have also determined the age of our programme stars from their locations in the HR diagram. We have made use of the Girardi et al. (2000) database of isochrones. For objects with near solar metallicity, the isochrones corresponding to z = 0.019 are adopted. These are illustrated in Figures 5, 6 and 7. The masses of HD 98893, HD 53199 are 3.5 M. The masses of HD 18182, HD 119185, HD 211594, and HD 40430 are 2.5 M. The above stars have higher than the verage mass of mild Ba stars (1.9 or 2.3 M) given by Han et al. (1995). The masses of HD 22589, HD 147609 HD 106191 and HD 150862 are 1.7 M $\odot$,1.4 M $\odot$ and 1.2 M $\odot$ respectively, which are consistent with the average mass 1.5 M $\odot$ of strong Ba star with 0.60 M $\odot$ companion white dwarfs given by Jorissen et al. (1998). The star HD 87080 is a strong Ba star as its mass 1.5 M which is same as the mass of strong Ba stars. The stars HD 106191 and HD 150862 are belonging to spectral type F and luminosity class v as their masses are 1.4 M $\odot$ 1.2 M $\odot$ as the stars of this type will have 1.0 to 1.4 solar masses.

The log g value is derived from the below formula,

$$\log \frac{g}{g_\odot} = \log \frac{M}{M_\odot} + 4\log \frac{T_{eff}}{T_{eff\odot}} + 0.4(M_{bol} - M_{bol\odot})$$

where the solar values are log g = 4.44, T eff =5770K and Mbol =4.75 and the effective temperature is calculated using the

infrared flux method, the stellar mass is calculated using the HR diagram and the bolometric mass is calculated by,

MB = Mv + BC–Av.

The star HD 150862 has the highest log g value of 4.07 cgs with an error of 0.30 and HD 134698 with least log g of 1.17 cgs with an error of 0.30.
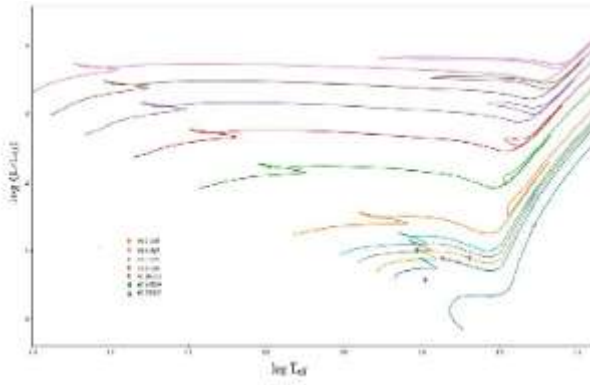
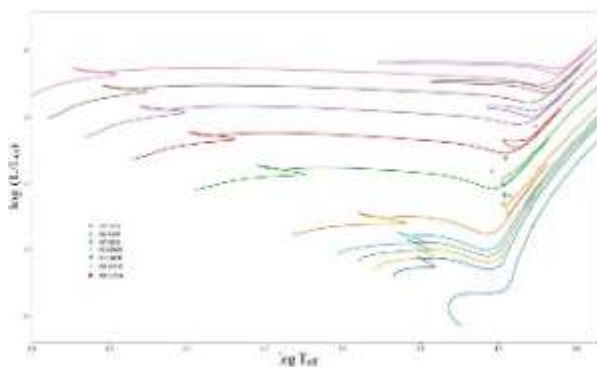Fig 3. The locations of HD 22589, HD 40430, HD 76225, HD

Fig 4. The locations of HD 18182, HD 53199, HD 98839, HD 119185, HD 134698, HD 193915, and HD 211594. The evolutionary tracks for 1.0, 1.4, 1.5, 1.6, 1.7, 2.0, 3.0, 4.0, 5.0, 6.0 and 7.0 M ⊙ are shown from bottom to top.

5.3 AGE

The age of our stars is calculated, and the trends are plotted with the isochrone lines. In the isochrones lines we can determine the information about the open cluster that a star is in. The data for trends are collected from the Padova online database (http://pleiadi.pd.astro.it/). Data of many other objects of similar age are plot- ted to analyze the trend that it will form. Age is one of the important variables in analyzing the evolutionary track of the stars. The fig 3 is used in determining the age of the stars. The star HD 150862 is the old star in our study and its age is around 3.36 Gyr and the star HD 183951 is the youngest star in our study it has an age of around 0.53 Gyr.

5.4 Metallicity Estimates

Equivalent widths of a set of clean and unblended Fe I and Fe II lines are used for the estimation of atmospheric parameters. The lines are selected to have the excitation

potential in the range 0.0 - 5.0 eV and the equivalent widths in the range 20 - 180 A˚. The number of Fe II lines measured on the spectra is smaller than the number of Fe I lines. We have made use of Local Thermodynamic Equilibrium (LTE) analysis of the measured equivalent widths using a recent version of radiative transfer code. Model atmospheres used are selected from Kurucz grid of model atmospheres with no convective overshooting (http://cfaku5.cfa.hardvard.edu/). Solar abundances are adopted from Asplund et al. (2009). The estimated abundances of Fe I and Fe II lines are used to derive the metallicity of the stars. The adopted atmospheric parameters are listed in Table 2.

5.5 Abundance Analysis

Abundance analysis of the stars are done by firstly crop- ping the full spectrum into many sections, each section covering about 50 in wavelength. The different sections are then continuum fitted for flux value of 1. Lines due to different elements are identified by overplotting the Arcturus spectra on the spectra of our programme stars. Only symmetric, clean lines are used for abundance analysis and the equivalent widths of these lines are measured. A master line list with the measured equivalent widths, and line information such as lower excitation potential and log g values of the lines due to different elements considered for abundance estimates is prepared using the Kurucz database. The lines having equivalent width less than 10m˚A are not considered being week and as the abundance estimates obtained from those lines may not be accurate. A master line list with the measured equivalent widths, and line information such as lower excitation potential and log g values of the lines due to different elements considered for abundance estimates is prepared using the Kurucz database. Then the spectra having the selected lines are synthesized using iSpec software for abundance calculation. MOOG code, using model atmospheres from ATLAS9, Castelli model atmosphere were also used. The line list used for abundance analysis is GESv5 atom hfs iso.420 920nm. The lower excitation potential, primary standard lists of the lines, log gf values are adopted from the Kurucz online database. The Solar Abundances used are adopted from Asplund 2009. The parameters and abundances were found out using spectral synthesis method. The values for Effective temperature, Metallicity, Surface gravity, microturbulence were given as input and the synthetic spectra were generated. After finding the absolute abundances of the

elements, the values of [X/H] and [X/Fe] are calculated using the given formula.

[X/H] = A(X)–[X/H].

[X/Fe] = [X/H]–[Fe/H].

The values obtained for the elements were recorded. Many lines due to each element were used whenever possible to get more accurate results. These values are tabulated I Tables xx through xxx. The lines for Fe1 and Fe2 were found out using the same method to verify the value used for [X/Fe]. The final average abundances of each element are estimated, and compared with their counterparts observed in other barium stars from literature.

Abundances of light elements, C, N O, odd-Z element Na, -and Fe-peak elements Mg, Si, Ca, Sc, Ti, V, Cr, Mn, Co, Ni and Zn are measured. Among the neutron-capture elements we have estimated the abundances of elements Sr, Y, Zr, Ba, La, Ce, Pr, Nd, Sm, and Eu. For elements. The abundance results are presented in Tables 5 through 10 and the lines used for the abundance determination are presented in Tables 11 through 16.

5.5.1 O, Na, Al

The oxygen triplets and sodium lines are observed and analysed for all the stars. The absolute abundances vary from 8-9. With the lowest value being 8.59 for the star HD183915 and highest being 9.02 for HD147609. The [O/Fe] value for HD134698 is 0.59 being the highest and the lowest [O/Fe] is 0.27 for the star HD98839. [Na/Fe] value for HD134698 is 0.44 which is the most sodium abundant star. The object HD 87080 however shows a mild underabundance with [Na/Fe] = 0.1. The abundance pattern of this star follows the abundance pattern of the disk stars which are having circular orbits in the plane of the galaxy and are quite young stars. Abundance pattern of alpha process elements, iron group, manganese, sodium is resembling the pattern of disk stars. We could not estimate Al abundance as no clear Al lines could be detected due to line blending. We have derived the O and Na abundances for all the program stars using strong lines in the spectra whenever available.

5.5.2 Mg, Ca, Sc, Ti

During the abundance analysis for elements like Ti, Ca many lines were found in out of which the best fitted lines are selected. Synthesis lines for magnesium were obtained

as one of the best synthesize fitted lines. The star HD95241 has [Mg/Fe] = 0.03 and [Ca/Fe] = 0.07 showing it has less abundance for these light elements. Stars HD98839 and HD147609 has under abundance while HD98839 being lowest under abundant star of [Mg/Fe] = -0.27. Some elements have shown over abundance like the object HD 134698 where [Mg/Fe] = 0.5 which is way more than the barium star limits of Mg (Yang et al. (2016) estimated a ratio of [Mg/Fe] 0.28 for the two barium stars HD 31308 and HD 224276). Abundance ratios of Ti with respect to iron are like those generally observed in normal giants and barium stars. But HD 134698 has a higher value of [Ti/Fe] =0.41. While Sc abundance ratios in three stars are like those observed in normal giants, HD 134698 shows a higher value with [Sc/Fe] = 0.37. Sc abundance ratios are well within the range seen in barium stars. Some under abundance values shows that there are some very mild barium stars.

5.5.3 Mn, Cu, Ni, Zn

The [Cu/Fe] for the objects HD15086 2, HD147609 are observed as -0.12, -0.10 respectively by Allen Barbuy (2006). The estimated value for [Cu/Fe] in our abundance analysis are -0.31, -0.44 respectively. Ni shows near solar value with [Ni/Fe] 0.07. Abundance ratios of iron peak elements exhibit similar values as seen in barium stars. However, a close agreement with the values of normal giants are not observed in all the cases. Cu abundances derived using Cu I lines show near solar values for HD 22589 (+0.07) and HD 211594 (0.15). Cu is overabundant in HD 183915 with [Cr/Fe] = 0.56 and under abundant in HD 98839 with [Cr/Fe] = 0.15. Cr abundances measured using Cr II lines whenever possible also give similar results. Mn abundance is obtained using spectrum synthesis calculation of 6013.51 ˚A line considering the hyperfine structures from Prochaska McWilliam (2000). Most objects were well within the barium limit close to solar values but HD 40430 (-0.46) and HD 98839 (-0.56) prove to be very underabundant. We could estimate Zn abundance in most objects, HD 183915 and HD 98839 using a Zn I line that gave [Zn/Fe] = -0.41 and -0.28 respectively which are lower than those normally seen in normal giants and barium stars.

5.5.4 Sr, Y, Zr

Sr is overabundant in HD 150862, HD 147609 with [Sr/Fe] values 0.86, 1.23 respectively. Some of the Sr II lines detected in the spectra are found suitable for abundance estimate but these stars already prove to be overabundant. Among the three-light s-process elements, Yang et al. (2016) and de Castro et al. (2016) have reported abundances only for Y and Zr. These values for HD 49641 and HD 58368 are respectively (Y: 0.35, 0.41; Zr: 0.41, 0.25; Yang et al.) and (Y: 0.89, 0.85; Zr: 0.53, 0.60; de Castro et al.). We could measure the abundance of Y in 10 most of the stars. Y is found to be significantly overabundant in HD

147609. Zr has shown overabundance in many objects like HD 22589, HD 87080 with a value of [Zr/Fe]=0.85 and 1.23, respectively. Some objects have shown near solar values for Zr.

5.5.5 Ba, La, Ce, Pr, Nd, Sm, Eu

Strong barium stars are the stars having [Ba/Fe] > 0.6. Stars having 0.17 < [Ba/Fe] < 0.54 are called as mild barium stars.

From our analysis, we found that stars HD22589, HD106191, HD147609, HD87080, HD183915, HD211594 are strong barium stars, and stars HD95241, HD134698, HD150862, HD76225, HD98839, HD119185 are mild barium stars. Many stars show over abundance from solar values which proves that these are Barium related stars but some stars like HD 40430 show [Ba/Fe] = 0.1 which shows that it is a like barium star or a CH subgiant. But other stars like HD 22589 have [Ba/Fe] = +1.33 showing a very strong barium star. Most of the objects are on the border of the limit of the barium star. HD 147609 has [X/Fe] > 0.89 (Y, La, Nd, Pr) but HD 87080 and HD183915 have [X/Fe]> 0.7(Y, La, Nd, Pr) showing a sight deviation.

VI. CONCLUSION

We have presented results obtained from high resolution spectroscopic analysis of 15 barium stars. All the programme stars except HD 134698, HD 18182 and HD 119185 are confirmed binaries with period ranging from 274 to 16471 days. We have determined the atmospheric parameters T-eff, logg, metallicity of the stars, and have estimated the elemental abundances of several elements such as O, Na, Mg, Ca, Ni, Sr, Y, Zr, Ba, La, Ce, Pr, Nd, Sm and Eu. Elemental abundances are determined by synthesizing the spectra of each star. The abundance of oxygen is estimated from spectral synthesis of oxygen triplets for all the stars and the absolute abundance values are found to range from 8.59 to 9.02. To obtain the metallicity values we have analysed the Fe I and Fe II lines in the star across different wavelengths in the spec tra. The metallicity values obtained by us are found to match closely with those available in literature. The lowest [Fe/H] value we have obtained is -1.41 for the star HD 150862 with an error of 0.10 dex. The highest [Fe/H] value is of -0.13 for the star HD 22589 with an error of 0.06 dex. We have estimated the mass of all the 15 program stars using the evolutionary tracks in the H-R diagram ($\log$(L/L $\odot$) vs T eff plot). The masses for the stars range from 1.20 M to 4.50

M $\odot$. The most massive of the stars is the HD 183915 and the least massive is HD 150862. The objects HD 22589, HD 40430, HD 76225, HD 87080, HD 106191, HD 147609, and HD 150862 are found to be in the main-sequence. The objects namely HD 183915, HD 98839, HD 53199, HD 119185, HD 134698, HD 211594, HD 18182 are found to be in the giant and subgiant phase of evolution. We have determined the age of the stars and the most aged star is HD 150862 being 3.36 Gyr. The youngest star is HD 183915 with 0.53 Gyr. We have com- pared the elemental abundances of our stars with their counterparts in other known barium stars from literature and found to be consistent.
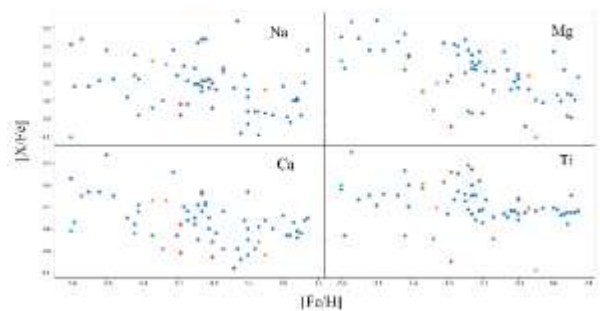
Fig 6. The Abundance ratio of the light elements (like Na, Mg, Ca, and Ti) from the programme stars are compared to [X/Fe] of the other barium stars obtained from Kuruz database.
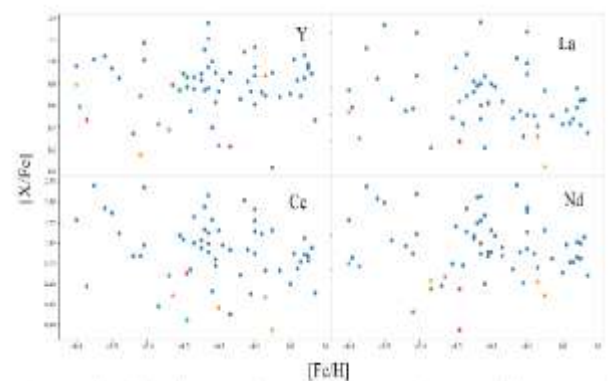
Fig 7. The Abundance ratio of the heavy elements (like Y, La, Ce, and Nd) from the programme stars are compared to [X/Fe] of the other barium stars obtained from Kuruz database.

Table 1: The photometric temperature estimates according to calibration equations of Alonso et al. (1999,2001), following procedures from Goswami et al. (2006,2016)

Star	Teff	Teff	Teff	Teff	Teff	Teff	Teff	Teff	Teff	Teff	Spectroscopic
Name	-0.05	-0.5	-1.5	-0.05	-0.5	-1.5	-0.05	-0.5	-1.5	estimates	
	(J–K)	(J–H)	(J–H)	(J–H)	(V–K)	(V–K)	(V–K)	(B–V)	(B–V)	(B–V)	
HD18182	4853.12	4762.89	4701.4	4510.25	4750.54	4762.8	4810.03	4671.08	4372.34	4131.14	4858
HD22589	5501.16	5805.96	5819.76	5850.65	5351.34	5340.92	5334.23	5411.24	5272.08	5067.06	5672
HD40430	4625.98	4781.78	4822.51	4943.12	4720.48	4705.59	4636.11	4771.27	4666.67	4530.77	4930
HD53199	5099.09	5234.732	5005.12	4785.77	4994.57	5006.57	5055.21	4785.46	4112.3	4012.73	5119
HD76225	4830.66	5035.57	5080.03	5110.49	4793.15	4776.795	4760.11	4790.42	4684.05	4545.03	6340
HD87080	5441.47	5691.8	5761.32	6369.81	5304.39	5295.55	5300.78	5258.58	5759.92	4884.19	5483
HD95241	7656.62	6902	6912.23	6935.08	-	-	-	-	-	-	5837
HD98839	4931.024	5572.31	5501.86	5232.5	4846.15	4834.53	4882.301	4771.82	4656.32	4424.93	4917
HD106191	5921.35	5572.31	5501.86	5232.5	4846.15	4834.53	4882.301	4771.82	4656.32	4424.93	5946
HD119185	4734.75	4886.5	4821.3	4619.61	4754.7	4800	4998.06	4969.23	4655.42	4165.28	4919
HD134698	4757.81	4329.41	4360.37	4274.29	4108.36	4091.82	4069.67	4563.51	4496.62	4390.35	4438
HD147609	3760.11	3535.49	3549.29	3580.35	5135.78	5319.93	5799.81	6165.46	5998.25	5760.42	6411
HD150862	6534.42	6352.01	6435.96	6504.9	6175.41	6184.58	6238.23	5978.65	5853.66	5675.19	6253
HD183915	4350.88	4670.99	4708.85	4729.39	4344.45	4352.52	4540.66	4181.88	4107.58	4014.1	4494
HD211594	4728.04	4996.93	4928.13	4716.07	4723.56	4735.87	4783.14	4441.5	4159.78	4012.73	4947

The numbers in the parenthesis below Teff indicate the metallicity values at which the temperatures are calculated. Temperatures are given in Kelvin.

Table 2: The metallicity of the star was calculated by finding the value of [X/H] of Fe I and Fe II. This was done in the same process used to find the elemental abundances.

Star	FeI			FeII		
Name	$\log\epsilon$	[X/H]	[X/Fe]	$\log\epsilon$	[X/H]	[X/Fe]
HD18182	7.23	-0.17	0.00	7.60	0.10	0.07
HD22589	7.37	-0.13	-0.06	7.42	-0.07	0.00
HD40430	7.13	-0.36	-0.02	7.04	-0.46	-0.12
HD53199	7.27	-0.23	-0.03	7.37	0.13	0.33
HD76225	7.09	-0.40	-0.03	7.23	-0.26	0.11
HD87080	6.63	-0.86	-0.26	6.74	-0.83	-0.23
HD95241	7.09	-0.41	-0.04	7.33	-0.19	0.29
HD98839	7.16	-0.33	-0.28	7.15	-0.31	-0.26
HD106191	7.22	-0.28	0.01	7.31	-0.19	0.10
HD119185	6.90	-0.60	-0.18	7.01	-0.49	-0.07
HD134698	6.92	-0.58	-0.01	7.10	-0.39	0.18
HD147609	7.24	-0.26	-0.03	7.46	-0.04	0.19
HD150862	2.41	-1.41	0.10	2.94	-2.64	0.08
HD183915	6.90	-0.59	0.00	6.92	-0.57	-0.01
HD211594	7.27	-0.23	-0.43	7.37	-0.13	-0.33

Table 3: Estimates of log g using parallax method.

Star Name	Parallax (mas)	M_{bol}	$\log(L/L_\odot)$	Mass $(M_\odot)$	log g (cgs)	log g (spectroscopic) (cgs)	Age (Gyr)
HD 18182	8.95 ± 0.04	2.58 ± 0.05	0.821 ± 0.009	2.50	2.89 ± 0.02	2.53 ± 0.36	0.80
HD 22589				1.65	2.61 ± 0.03	2.88 ± 0.18	2.51
HD 40430	2.81 ± 0.04	0.48 ± 0.002	1.82 ± 0.008	2.50	2.74 ± 0.02	2.44 ± 0.18	0.80
HD 53199				3.50			0.63
HD 76225	5.89 ± 0.03	2.06 ± 0.002	1.07 ± 0.01	1.65	4.09 ± 0.10	3.88 ± 0.10	1.26
HD 87080	4.58 ± 0.07	0.18 ± 0.02	0.89 ± 0.007	1.50	3.63 ± 0.0003	3.62 ± 0.31	2.15
HD 95241	21.28 ± 0.15	-	-	-	-	3.63 ± 0.15	-
HD 98839	5.87 ± 0.19	−1.22 ± 0.001	2.39 ± 0.03	3.50	2.31 ± 0.03	2.30 ± 0.55	0.60
HD 106191	6.43 ± 0.19	2.54 ± 0.07	0.89 ± 0.03	1.40	3.75 ± 0.03	4.31 ± 0.44	2.15
HD 119185	2.04 ± 0.05	0.69 ± 0.05	1.84 ± 0.02	2.50	2.93 ± 0.02	2.5 ± 0.00	0.80
HD 134698	1.65 ± 0.06	−0.25 ± 0.07	1.99 ± 0.03	1.70	2.22 ± 0.03	1.17 ± 0.30	0.80
HD 147609	4.30 ± 0.11	2.25 ± 0.05	0.99 ± 0.02	1.65	3.84 ± 0.02	3.9 ± 0.50	1.34
HD 150862	8.86 ± 0.14	3.32 ± 0.0001	0.56 ± 0.008	1.20	3.75 ± 0.04	4.07 ± 0.30	3.36
HD 183915	2.79 ± 0.04	−2.43 ± 0.0002	2.86 ± 0.03	4.50	1.79 ± 0.05	1.55 ± 0.35	0.53
HD 211594	3.58 ± 0.07	0.80 ± 0.08	1.69 ± 0.02	2.50	2.97 ± 0.02	2.60 ± 0.13	0.80

Table4: Elemental Abundances for HD 18182, HD 22589, HD 40430 and HD 53199

ELEMENT	(Z)	Solarlog(ε)	HD18182[X/H]			HD22589		
			logε	[X/H]	[X/Fe]	logε	[X/H]	[X/Fe]
OI	8	8.69	8.7	0.01	0.18	8.88	0.19	0.26
NaI	11	6.24	6.32	0.09	0.26	6.19	-0.05	0.04
MgI	12	7.60	7.47	-0.12	0.04	7.66	0.07	0.14
Ca I	20	6.34	6.18	-0.15	0.01	6.31	-0.03	0.04
Sc II	21	3.15	3.15	0	0.17	3.28	0.13	0.20
TiII	22	4.95	4.59	-0.36	-0.19	4.89	-0.05	0.02
MnI	25	5.43	5.03	-0.39	-0.22	5.47	0.04	0.01
NiI	28	6.22	5.82	-0.38	-0.21	6.21	-0.01	0.06
CuI	29	4.19	3.98	-0.21	-0.04	6.22	0.00	0.07
ZnI	30	4.56	4.36	-0.2	-0.03	4.51	-0.04	0.03
SrI	38	2.87	2.93	0.06	0.23	3.26	0.40	0.47
SrII	38	2.87	-	-	-	3.17	0.30	0.37
YII	39	2.21	2.26	0.06	0.23	3.01	0.80	0.87
Zr II	40	2.58	2.18	0	0.17	3.36	0.78	0.85
BaII	56	2.18	2.56	0.38	0.55	3.43	1.26	1.33
LaII	57	1.10	1.13	0.03	0.2	1.62	0.52	0.59
CeII	58	1.58	1.48	0.03	0.13	1.84	0.27	0.34
NdII	60	1.42	1.46	0.04	0.21	1.67	0.26	0.33
PrI	59	0.72	0.64	-0.08	0.09	0.84	0.13	0.20
SmII	62	0.96	-	-	-	1.04	0.08	0.15

ELEMENT (Z)		Solarlog(ϵ)	HD 40430			HD 53199		
EuII	63	0.52	-	-	-	0.52	0.00	0.07

ELEMENT (Z)		Solarlog(ϵ)	HD 40430			HD 53199		
			logϵ	[X/H]	[X/Fe]	logϵ	[X/H]	[X/Fe]
OI	8	8.69	8.61	-0.08	0.26	8.89	0.2	0.4
NaI	11	6.24	6.00	-0.24	0.10	6.24	0.005	0.2
MgI	12	7.60	7.23	-0.36	-0.09	7.28	-0.31	-0.11
Ca I	20	6.34	6.01	-0.33	0.01	6.1	-0.23	-0.03
Sc II	21	3.15	3.06	-0.09	0.25	3.04	-0.1	0.09
TiII	22	4.95	4.41	-0.53	-0.19	4.48	-0.28	-0.08
MnI	25	5.43	4.63	-0.80	-0.46	4.86	-0.57	-0.37
NiI	28	6.22	3.72	-0.47	-0.13	5.78	-0.43	-0.23
CuI	29	4.19	5.39	-0.65	-0.31	3.67	-0.51	-0.31
ZnI	30	4.56	3.72	-0.47	-0.13	4.01	-0.49	-0.29
SrI	38	2.87	3.87	-0.69	-0.35	3.1	0.23	0.43
SrII	38	2.87	2.66	-0.21	0.13	-	-	-
YII	39	2.21	2.25	0.04	0.38	2.25	0.04	0.24
Zr II	40	2.58	2.82	0.24	0.58	3.06	0.49	0.69
BaII	56	2.18	1.93	-0.25	0.10	2.82	0.65	0.85
LaII	57	1.10	-	-	-	1.93	0.06	0.26
CeII	58	1.58	1.35	0.26	0.60	2.08	0.5	0.71
NdII	60	1.42	1.35	0.07	0.27	1.99	0.57	0.77
PrI	59	0.72	0.78	0.06	0.40	1	0.28	0.48
SmII	62	0.96	0.91	-0.04	0.30	-	-	-
EuII	63	0.52	0.55	0.03	0.37	-	-	-

*   Referenceforsolarabundances:Asplundetal2009

Table5:Elemental Abundances for HD 76225, HD 87080, HD 95241and HD 988839

ELEMENT (Z)		Solarlog(ϵ)	HD76225[X/H]			HD87080[X/H]		
			logϵ		[X/Fe]	logϵ		[X/Fe]
OI	8	8.69	8.72	0.04	0.41	8.66	-0.04	0.56
NaI	11	6.24	6.18	-0.06	0.32	5.73	-0.51	-0.10
MgI	12	7.60	7.26	-0.34	0.04	7.21	-0.37	0.24
Ca I	20	6.34	6.20	-0.14	0.23	5.78	-0.56	0.09
Sc II	21	3.15	3.08	-0.07	0.30	2.85	-0.30	0.30
TiII	22	4.95	4.76	-0.18	0.19	4.53	-0.42	0.18
MnI	25	5.43	4.96	-0.31	0.06	4.60	-0.82	-0.23
NiI	28	6.22	5.83	-0.38	-0.01	5.38	-0.84	-0.24
CuI	29	4.19	3.90	-0.29	0.08	3.29	-0.90	-0.30
ZnI	30	4.56	4.28	-0.28	0.09	3.92	-0.64	-0.04
SrI	38	2.87	2.92	0.05	0.42	3.16	0.29	0.89
SrII	38	2.87	2.94	0.07	0.44	2.88	0.02	0.62

YII	39	2.21	2.27	0.06	0.43	2.39	0.19	0.79
Zr II	40	2.58	2.60	0.07	0.39	3.20	0.63	1.23
BaII	56	2.18	2.29	0.11	0.48	2.18	0.00	0.60
LaII	57	1.10	-	-	-	1.53	0.44	1.04
CeII	58	1.58	-	-	-	-	-	-
NdII	60	1.42	1.40	0.02	0.35	1.42	0.00	0.60
PrI	59	0.72	0.81	0.09	0.46	1.19	0.47	1.07
SmII	62	0.96	1.11	0.16	0.53	1.20	0.24	0.84
EuII	63	0.52	0.50	-0.02	0.35	0.81	0.29	0.89

ELEMENT	(Z)	Solarlog(ϵ)	HD 95241			HD 98839		
			logϵ	[X/H]	[X/Fe]	logϵ	[X/H]	[X/Fe]
OI	8	8.69	8.68	0.02	0.39	8.91	0.22	0.27
NaI	11	6.24	5.92	-0.31	0.06	6.35	0.11	0.16
MgI	12	7.60	7.26	-0.34	0.03	7.27	-0.32	-0.27
Ca I	20	6.34	6.03	-0.30	0.07	6.26	-0.07	-0.02
Sc II	21	3.15	2.88	-0.27	0.11	3.03	-0.11	-0.06
TiII	22	4.95	4.73	-0.21	0.16	4.48	-0.46	-0.41
MnI	25	5.43	4.96	-0.46	-0.09	4.81	-0.61	-0.56
NiI	28	6.22	5.93	-0.29	0.08	5.89	-0.31	-0.26
CuI	29	4.19	3.39	-0.80	-0.43	3.65	-0.53	-0.48
ZnI	30	4.56	4.11	-0.44	-0.07	4.23	-0.33	-0.28
SrI	38	2.87	2.39	-0.48	-0.11	2.44	-0.42	-0.37
SrII	38	2.87	2.57	-0.29	0.08	-	-	-
YII	39	2.21	1.89	-0.31	-0.68	2.2	-0.01	0.04
Zr II	40	2.58	2.24	-0.34	0.04	1.59	-0.99	-0.94
BaII	56	2.18	2.21	0.03	0.40	2.34	0.17	0.22
LaII	57	1.10	1.11	0.01	0.38	1.08	-0.02	0.03
CeII	58	1.58	1.41	-0.15	0.23	0.69	-0.11	-0.06
NdII	60	1.42	1.27	-0.14	0.23	1.49	0.08	0.13
PrI	59	0.72	-	-	-	0.71	0	0.05
SmII	62	0.96	0.53	-0.43	-0.06	-	-	-
EuII	63	0.52	0.69	0.17	0.54	-	-	-

Reference for solar abundances: As plund et a l2009

Table 6: Elemental Abundances for HD 106191, HD 119185, HD 134698 and HD 147609

ELEMENT (Z)		Solarlog(ϵ)	HD 106191			HD 119185		
			logϵ	[X/H]	[X/Fe]	logϵ	[X/H]	[X/Fe]
OI	8	8.69	8.69	0.00	0.29	8.77	0.09	0.51
NaI	11	6.24	6.03	-0.21	0.08	6.16	-0.07	0.35
MgI	12	7.60	7.45	-0.15	0.14	7.34	-0.25	0.16
CaI	20	6.34	6.16	-0.17	0.12	6.03	-0.3	0.11
ScII	21	3.15	3.17	0.03	0.32	2.82	-0.32	0.09
Ti II	22	4.95	4.93	-0.02	0.27	4.48	-0.46	-0.04
MnI	25	5.43	5.22	-0.20	0.09	4.78	-0.64	-0.22
NiI	28	6.22	6.02	-0.20	0.10	5.56	-0.65	-0.23
CuI	29	4.19	4.05	-0.14	0.15	3.76	-0.42	-0.005
Zn I	30	4.56	4.35	-0.21	0.08	4.19	-0.36	0.06
SrI	38	2.87	3.20	0.33	0.62	2.85	-0.02	0.4
SrII	38	2.87	-	-	-	-	-	-
YII	39	2.21	2.69	0.48	0.77	2.07	-0.14	0.28
ZrII	40	2.58	2.21	0.00	0.29	2.65	0.08	0.5
BaII	56	2.18	2.89	0.72	1.01	2.34	0.16	0.58
LaII	57	1.10	1.31	0.21	0.50	1.26	0.16	0.58
CeII	58	1.58	1.92	0.34	0.63	1.72	0.14	0.56
NdII	60	1.42	1.35	-0.07	0.23	1.59	0.18	0.6
PrI	59	0.72	0.73	0.01	0.30	0.7	-0.02	0.4
SmII	62	0.96	0.97	0.01	0.30	-	-	-
EuII	63	0.52	0.52	0.01	0.30	-	-	-

ELEMENT (Z)		Solarlog(ϵ)	HD134698			HD147609		
			logϵ	[X/H]	[X/Fe]	logϵ	[X/H]	[X/Fe]
OI	8	8.69	8.71	0.02	0.59	9.02	0.33	0.56
Na I	11	6.24	6.10	-0.13	0.44	6.22	-0.02	0.21
MgI	12	7.60	7.53	-0.07	0.50	7.48	-0.13	-0.11
CaI	20	6.34	6.01	-0.32	0.25	6.30	0.04	0.27
ScII	21	3.15	2.95	-0.20	0.37	3.10	-0.05	0.18
Ti II	22	4.95	4.79	-0.16	0.41	5.02	0.004	0.29
MnI	25	5.43	4.94	-0.49	0.08	5.25	-0.18	0.05
NiI	28	6.22	5.82	-0.40	0.17	6.05	-0.16	0.07
CuI	29	4.19	4.12	-0.07	0.50	3.52	-0.67	-0.44
Zn I	30	4.56	4.02	-0.54	0.03	4.40	-0.16	0.07
SrI	38	2.87	2.80	-0.06	0.51	3.87	1.00	1.23
SrII	38	2.87	-	-	-	3.22	0.35	0.58
YII	39	2.21	2.11	-0.10	0.47	3.19	0.98	1.21
ZrII	40	2.58	2.60	0.02	0.59	3.16	0.58	0.81
BaII	56	2.18	2.12	-0.06	0.51	2.92	0.74	0.97
LaII	57	1.10	1.08	-0.02	0.55	2.00	0.91	1.17

CeII	58	1.58	1.47	-0.11	0.47	2.49	0.91	0.99
NdII	60	1.42	-3.30	-0.03	0.55	2.08	0.67	0.89
PrI	59	0.72	0.61	-0.11	0.46	1.54	0.82	1.05
SmII	62	0.96	0.85	-0.11	0.47	1.80	0.85	1.08
Eu II	63	0.52	0.35	-0.17	0.40	-	-	-

*   Reference for solar abundances: Asplund etal 2009

Table 7: Elemental Abundances for HD 150862, HD 183915, and HD 221594

ELEMENT	(Z)	Solarlog(ϵ)	logϵ	HD 150862[X/H]	[X/Fe]	logϵ	HD 183915[X/H]	[X/Fe]
OI	8	8.69	8.88	0.19	0.52	8.59	-0.10	0.49
NaI	11	6.24	6.21	-0.03	0.30	5.83	-0.41	0.18
MgI	12	7.60	7.36	-0.24	0.09	7.19	-0.41	0.19
CaI	20	6.34	6.24	-0.10	0.23	5.87	-0.46	0.13
ScII	21	3.15	3.10	-0.05	0.28	2.48	-0.67	-0.08
Ti II	22	4.95	4.64	-0.31	0.02	4.19	-0.76	-0.17
MnI	25	5.43	5.14	-0.29	0.04	4.78	-0.65	-0.06
NiI	28	6.22	5.74	-0.48	-0.15	5.52	-0.71	-0.12
CuI	29	4.19	3.55	-0.64	-0.31	4.16	-0.03	0.56
Zn I	30	4.56	4.36	-0.20	0.13	3.55	-1.00	-0.41
SrI	38	2.87	3.40	0.53	0.86	2.48	-0.39	0.20
SrII	38	2.87	3.32	0.45	0.78	-	-	-
YII	39	2.21	2.67	0.46	0.79	2.20	0.00	0.59
ZrII	40	2.58	3.01	0.43	0.76	2.54	-0.04	0.55
BaII	56	2.18	2.22	0.04	0.37	2.19	0.01	0.60
LaII	57	1.10	-	-	-	1.63	0.54	1.13
CeII	58	1.58	1.61	0.03	0.36	-	-	-
NdII	60	1.42	1.49	0.07	0.40	1.50	0.09	0.68
PrI	59	0.72	0.73	0.01	0.34	0.98	0.27	0.86
SmII	62	0.96	0.99	0.03	0.36	1.17	0.23	0.82
EuII	63	0.52	0.12	-0.40	-0.07	0.54	0.03	0.61

ELEMENT	(Z)	Solarlog(ϵ)	logϵ	HD211594 [X/H]	[X/Fe]
OI	8	8.69	8.84	0.15	0.44
NaI	11	6.24	6.22	-0.01	0.27
MgI	12	7.60	7.34	-0.25	0.03
Ca I	20	6.34	5.94	-0.39	-0.1
ScII	21	3.15	2.94	-0.2	0.08
TiII	22	4.95	4.57	-0.36	-0.07
MnI	25	5.43	4.6	-0.82	-0.53
NiI	28	6.22	5.81	-0.39	-0.1
Cu I	29	4.19	4.01	-0.18	0.11
ZnI	30	4.56	4.11	-0.44	-0.15
SrI	38	2.87	3.38	0.51	0.8
SrII	38	2.87	-	-	-
YII	39	2.21	2.38	0.18	0.47
ZrII	40	2.58	3	0.82	1.11
BaII	56	2.18	1.88	0.32	0.61

LaII	57	1.10	2.24	0.66	0.95
CeII	58	1.58	2.36	0.79	1.08
NdII	60	1.42	1.97	0.56	0.85
PrI	59	0.72	1.31	0.59	0.88
SmII	62	0.96	-	-	-
EuII	63	0.52	-	-	-

Reference for solar abundances: Asplund et al 2009

Table 8: Basic data for the programme stars.

Star Name	T_{eff}(K)	logg (cgs)	ζ (Kms^{-1})	[FeI/H]	[FeII/H]	Ref
HD18182	4858	2.53	1.3	-0.17	0.1	1
	4858	2.50	-	-0.17	-	2
HD22589	5672	3.73	1.2	-0.13	-0.07	1
	5400	3.30	1.1	-0.12	-0.27	3
	5600	3.80	1.4	-0.16	-	4
HD40430	4930	2.74	1.39	-0.36	-0.46	1
	4930	2.40	1.67	-0.34	-	2
HD53199	6340	2.61	1.37	-0.23	0.13	1
	5119	2.90	3.3	-0.2	-	2
HD76225	6340	4.09	1.3	-0.4	0.26	1
	6110	3.80	1.4	-0.34	-0.31	3
HD87080	5483	3.63	1.2	-0.86	-0.83	1
	5460	3.70	1	-0.49	-0.44	3
	5600	4.00	-0.51	1.2	-	5
HD95241	5837	-	1.36	-0.41	-0.19	1
HD98839	4917	2.31	1.56	-0.33	-0.31	1
	4917	2.30	3.86	-0.05	-	2
HD106191	5946	3.75	1.21	-0.28	-0.19	1
	5890	4.20	1.1	-0.22	-0.29	3
HD119185	4919	2.93	1.42	-0.6	-0.49	1
	4919	2.50	-	-0.42	-	2
HD134698	4438	2.22	1.62	-0.58	-0.39	1
	4438	1.70	-	-0.57	-	2
HD147609	6411	3.84	1.26	-0.26	-0.04	1
	5960	4.42	1.5	-0.45	0.08	3
HD150862	6253	3.75	0.94	-1.41	-2.64	1
	6310	4.60	1.4	-0.11	-0.1	3
HD183915	4494	1.79	1.55	-0.59	-0.57	1
	4382	1.60	0.56	-0.59	-	2
HD211594	4947	2.97	1.48	-0.23	-0.13	1
	4947	2.60	4.1	-0.29	-	2

Note. Reference: 1. Our Work, 2. Jorissen et al (2019), 3.Allen et al (2006), 4.Pereira (2005), 5.Pereira et al (2003)

VII. REFERENCES

[1]. Alvarez, R. Plez, B. 1998, AA, 330, 1109
[2]. Escorza, A., Karinkuzhi, D., Jorissen, A., et al. 2019, AA, 626, 128
[3]. Jorissen, A., Boffin, H. M. J., Karinkuzhi, D., et al. 2019, AA, 626, A127
[4]. Masseron, T., Merle, T., Hawkins, K. 2016, BACCHUS: Brussels AutomaticCode for Characterizing High accU- racy Spectra, Astrophysics Source Code Library, 1605.004 Plez, B. 2012, Turbo spectrum: Code for spectral synthe sis, Astrophysics Source Code Library, 1205.004
[5]. Raskin, G., van Winckel, H., Hensberge, H., et al. 2011, AA, 526, A69
[6]. Jorissen et al (2019), Allen et al (2006), Pereira (2005), Pereira et al (2003)
[7]. Asplund et al 2009.
[8]. Model atmospheres used are selected from Kurucz

grid of model atmospheres with no convective overshooting (http://cfaku5.cfa.hardvard.edu/).

[9]. High-resolution spectra for the objects under this study were acquired using the HERMES spectrograph (Raskin 2011) mounted on the 1.2m Mercator telescope at the Roque de los Muchachos Observatory, La Palma, Canary Islands.